# Universality class of the Mott transition in two dimensions

S. Moukouri
*Racah Institute of Physics, Hebrew University, Jerusalem 91904, Israel*

E. Eidelstein
*Department of Physics, NRCN, P.O. Box 9001, IL Beer-Sheva, 84190, Israel*

(Received 4 July 2012; published 8 October 2012)

We use the two-step density-matrix renormalization group method to elucidate the long-standing issue of the universality class of the Mott transition in the Hubbard model in two dimensions. We studied a spatially anisotropic two-dimensional Hubbard model with a nonperfectly nested Fermi surface at half-filling. We find that unlike the pure one-dimensional case where there is no metallic phase, the quasi-one-dimensional model displays a genuine metal-insulator transition at a finite value of the interaction. The critical exponent of the correlation length is found to be $\nu \approx 1.0$. This implies that the fermionic Mott transition belongs to the universality class of the 2D Ising model.

DOI: 10.1103/PhysRevB.86.155112 PACS number(s): 71.30.+h, 71.10.Fd

## I. INTRODUCTION

In the studies of the Mott transition[1,2] in the ground state of the Hubbard model,[3] there are well controlled results in the pure one-dimensional (1D) case[4] and in the limit of infinite dimensions[5–7] only. In 1D, there is no metallic phase, the Mott gap opens as soon as the interaction $U > 0$. In infinite dimensions, the dynamical mean-field theory, which exactly predicts a Mott transition at the critical coupling, $U_c \approx W$, $W$ is the bandwidth. However, the transition has mean-field critical exponents. This anomaly is due to the local nature of the infinite-dimensional solution. Hence the one-dimensional and the infinite-dimensional solutions may not be directly applicable to experiments. Studies of the Mott transition in the Hubbard beyond these special limits of one dimension and infinite dimension are thus of crucial importance.

For more than a decade, a great deal of effort has been devoted to applying quantum cluster theories[8–14] to the study of the Mott transition in the Hubbard model in two dimensions (2D). Quantum cluster theories include nonlocal correlations. They predict a finite critical value for the interaction at the transition. This critical value depends on the cluster size. However, when applied to a finite dimensional model, they are exact only in the limit of infinite cluster size. In quantum cluster theories, the effect of the interaction on physical quantities such as the single-particle Green's function is restricted to the cluster sites. The correlations are fully accounted for distances that are smaller than the cluster length, $r \lesssim L_c$. When $r \gtrsim L_c$, the Green's function has an effective mean-field decay. Restricting the effect of the interaction at distances $r \lesssim L_c$ is probably justified away enough from the critical point where the correlations are expected to be short ranged. A consequence of this restriction of the correlations to the cluster length is that the exponents at the transition are always mean-field like for a fixed cluster size.[10] A systematic finite cluster size analysis is therefore necessary for a correct description of the transition. However, most of applications of quantum cluster simulations have been done on relatively small clusters. These are not enough to reliably predict the low-energy physics at the quantum critical point.

Unlike the fermionic model, in the 2D Bose-Hubbard model, which displays a transition from a superfluid to a Mott insulator, analytical approaches[15,16] and large scale Monte Carlo simulations[17] have yielded reliable information about its critical behavior. The transition for fixed boson density belongs to the universality class of the classical three-dimensional (3D) $XY$ model. This has also been reported on the 2D Jaynes-Cummings-Hubbard model.[18] Unfortunately, for the fermionic Hubbard model, Monte Carlo simulations predict $U_c = 0$. This is because of the nesting induced Slater transition.[19,20] In absence of perfect nesting, the Monte Carlo method is hampered by the sign problem. Large scale simulations are not possible.

Recent interest has been raised by slave rotor analyses.[21,22] These analyses suggest that the transition in the 2D fermionic Hubbard model may belong to the 3D $XY$ universality class as the bosonic Hubbard model. In Refs. 21 and 22, a slave rotor representation of the fermionic operator $c_{i\sigma} = b_i f_{i\sigma}$, where $b_i$ is a spinless boson and $f_{i\sigma}$ a charge-less spin, was used to map the Hubbard model to a free spinon Hamiltonian self-consistently coupled to a bosonic term (or $XY$ term in a spin representation of bosons). The fermionic Mott transition is in this form a transition between condensed (Fermi liquid) and noncondensed (Mott insulator) phases of bosons. This factorization may be justified in the Mott phase where, because of the Mott gap, spin, and charge degrees of freedom may be separated. However, as the critical point is approached, is the gauge field weak enough to justify the decoupling between spin and charge? If not, would that modify the critical behavior predicted by the slave-rotor approximation? Only a nonbiased calculation of the Hubbard model can yield the answer.

The slave-rotor prediction is in disagreement with an earlier approximate mapping[23] of the Hubbard model to a generalized Blume-Emery-Griffiths model[24] of the $H_e^3$-$H_e^4$ mixtures with an additional term whose effect on the nature of the transition is not known. In this mapping, doubly occupied and empty sites corresponds to $H_e^3$ sites and singly occupied sites to $H_e^4$ sites. This mapping suggests instead that the Hubbard model is in the universality class of the Ising model. But the extra term which accompanies the Blume-Emery-Griffiths model could well lead to another universality class.

 

In a recent paper,[25] we reported a two-step density-matrix renormalization group (DMRG)[26] study of the Mott transition in the ground state of the quasi-one-dimensional (1D) Hubbard model at half-filling. We find that in contrast to the pure 1D case for which there is no metallic phase, there is an authentic Mott transition in the quasi-1D model. However, it is possible to argue that in the quasi-1D dimensional Hubbard model studied in Ref. 25, the Fermi surface is perfectly nested, thus our analysis which predicts a gapless phase in the weak-coupling regime, would miss an exponentially small gap $\Delta \propto \exp -\frac{2\pi t}{U}$, that would open as a consequence of a Slater transition. However, our numerical data did not support the existence of such a gap. Arguments supporting a gap opening induced by perfect nesting are perturbative: the divergence of the noninteracting susceptibility $\chi_0(\mathbf{q})$ at the nesting wave vector leads to that of the interacting spin susceptibility, $\chi_s(\mathbf{q}) \propto 1/[1 - U\chi_0(\mathbf{q})]$. However, the actual susceptibilities and interaction in the expression of $\chi_s(\mathbf{q})$ are renormalized. Attempts to compute the renormalized susceptibilities and interaction within the self-consistent parquet formalism[27] lead to intractable equations. Hence the effect of these renormalization effects on the mean-field solution remains an open problem.

In this paper, we present a well controlled study of the Mott transition in the Hubbard model with a nonperfectly nested Fermi surface beyond the special cases of 1D and infinite dimensions. The choice of the nonperfectly nested Fermi surface precludes the theoretical possibility of a gap induced by the Slater anti-ferromagnetism mechanism. The two-step DMRG method is first checked on the transition between a paramagnetic and an anti-ferromagnetic ground states in the quasi-1D Heisenberg model with $S = 1$. In agreement with a quantum Monte carlo study,[28] we find that this transition belongs to universality class of the 3D classical Heisenberg model. For the quasi-1D Hubbard model, we find that, in contrast to the pure one-dimensional model, there is a genuine ground-state Mott transition at a finite critical value of the interaction. Data analysis of the critical behavior of this model show that, in agreement with the mapping to the Blume-Emery-Griffiths model,[23] the Mott transition in the 2D Hubbard model belongs to the universality class of the 2D Ising model. Hence our study shows the importance of studying quasi-1D models. These models are not only directly relevant for the physics of highly anisotropic materials, but they also yield crucial information about the isotropic models as well.

## II. MODEL

We consider the Hubbard model with the local interaction $U$ and the following noninteracting single-particle energies:

$$\epsilon(k_x,k_y) = -2t_x \cos k_x - 2t_y \cos k_y - 2t_d \cos(k_x + k_y) - 2t_d \cos(k_x - k_y), \quad (1)$$

the hopping parameters $t_x$, $t_y$, and $t_d$, respectively, in the longitudinal, transverse, and diagonal directions, are illustrated in Fig. 1. The presence of $t_d$ ensures that the noninteracting Fermi surface is not perfectly nested. $t_y$ and $t_d$ must be $(t_y,t_d) \ll t_x$ for the two-step DMRG method to be accurate. In this study, we set $t_x = 1$ and $t_y = t_d = 0.05t_x$. The choice of this model thus precludes the theoretical possibility of the nesting induced exponentially small gap. The bandwidth is $W = 4.4t_x$, we set $u = U/W$.

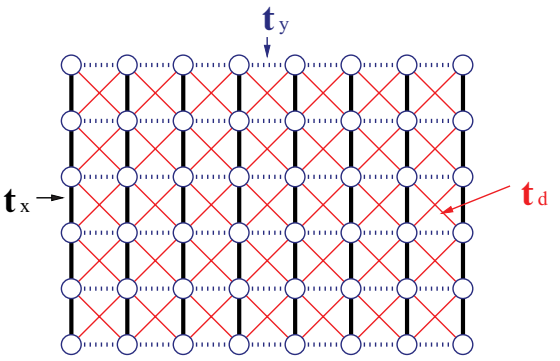


FIG. 1. (Color online) The anisotropic frustrated lattice with longitudinal $t_x$, transverse $t_y$, and diagonal $t_d$ hopping parameters.

## III. TWO-STEP DENSITY-MATRIX RENORMALIZATION GROUP

The two-step DMRG is a generalization of the conventional DMRG method[29] to quasi-1D Hamiltonians. The DMRG is a RG procedure in which the reduced density-matrix is used to retain the most important states of the system. The DMRG itself is a crucial improvement over the block RG method,[30] which extended the Wilson RG method[31] used in the solution of the Kondo impurity problem to lattice models. The block method has a major handicap, by dividing the lattice into independent blocks, it neglects at its initial step the interblock interaction. But if the interblock interaction is of the same order as the intrablock interaction, this introduces an error from which it is difficult to recover even by keeping a large number of states. In the DMRG, the lattice is built by initially coupling the block to the rest of the lattice. Let us consider a system (S) coupled to an environment (E), let $N_s$ and $N_e$ be, respectively, the number of states respectively of the system and for the environment. Let $\Phi$ be for instance the ground-state wave function of the supersystem including the system and the environment,

$$\Phi(S,E) = \sum_{i_s=1,N_s;i_e=1,N_e} \alpha_{i_s,i_e} \psi_{i_s} \chi_{i_e}, \quad (2)$$

where the $\psi_{i_s}$'s represent the system's basis states and the $\chi_{i_e}$'s the environment basis states; $N_s$ and $N_e$ are respectively the total number of states of the system and of the environment. The essence of the RG procedure is the truncation of the Hilbert's space, starting with a small system for which the total number of states can be kept, at some step when the lattice gets large, only a smaller number $m_s < N_s$ of the system's states can be kept. The error in this truncation is given by the eigenvalues $\lambda_{i_s}$ of the reduced density matrix of the system,

$$D_S = \sum_{i_e=1,N_e} \Phi(S,E)\Phi^*(S,E). \quad (3)$$

From the relation

$$\sum_{i_s=1,N_s} \lambda_{i_s} = 1, \quad (4)$$

the error made by representing the system by $m_s$ states instead of $N_s$ is given by

$$\rho = 1 - \sum_{i_s=1,m_s} \lambda_{i_s}. \tag{5}$$

For a large number of 1D models, $\rho$ is very small if $m_s$ is only a few hundreds. Application of the DMRG method to Heisenberg chains with $S = 1/2$ or $S = 1$,[29] $m_s \lesssim 100$, the ground-state energy, correlation functions, and lowest excitation gap were obtained with an astonishing accuracy.

It was hoped that, given the level of accuracy of the DMRG for 1D models, the method would also perform reasonably well for 2D models. However, for a 2D lattice, the value of $m_s$ necessary to retain good accuracy appears to increase exponentially with the system size. This is related to the entropy area law which predicts an exponential increase of $m_s \propto 2^{L^{D-1}}$ in 2D. The entropy area law implies that the direct application of the 2D DMRG would only be limited to relatively narrow systems, it however leaves a window of success for quasi-1D systems as we will explain below. The study of quasi-1D models would yield valuable information about the corresponding isotropic models. Most importantly, the two-step approach had a direct relevance to the physical properties of quasi-1D materials for which $t_y \ll t_x$ such as the organic and inorganic quasi-1D conductors.

Let us consider for instance the Hubbard chain with a charge gap $\Delta$. If the transverse coupling $t_y$ is infinitely small with respect to $\Delta$, so that the system remains in the same phase as the decoupled chains. It is obvious that the decoupled chain limit is a good starting point to describe the weakly coupled chain system. As $t_y$ increases, the quality of decoupled chain as a starting point will decrease, if the same number of states is kept, until $t_y$ reaches a quantum critical point $t_y^c$ at which the systems enters in the 2D regime. In principle, when $t_y$ is in the 2D phase, it would be wrong to start from the decoupled chain limit. This is because there are a huge number of low-lying states with nearly equal weight in the reduced density-matrix.

The important point which nevertheless makes calculations possible is that actual calculations are done on finite systems which have a discrete spectrum. Thus even if $t_y$ has a value corresponding to the 2D phase for a system size $L$, given the discreteness of the energy spectrum for a finite system, if the energy width of the states kept is such that $\Delta E \gg t_y$, starting from decoupled chain might still lead to accurate results. For such a system, the DMRG can be used to study the ground-state phase transition since it will display a different scaling behavior above and below $t_y^c$. The same type of analysis may be used for gapless chains as well, $\Delta(L)$ will yield the relevant energy scale above and below the transition.

The separation of the energy scales is basic idea of the two-step DMRG.[26] The two-step DMRG uses the extraordinary accuracy that the DMRG can achieve in 1D in two steps. In the first step, the low-energy Hamiltonian is obtained accurately using the DMRG. Then, in the next step small transverse perturbations are inserted. The 2D effective Hamiltonian is 1D, the DMRG is again applied to solve the problem in the transverse direction. Indeed, this procedure is valid only if the transverse couplings are very small with respect to the longitudinal couplings. The success of the two-step DMRG in yielding reliable results on the eventual new physics induced by the perturbation will depend on the value of the critical transverse coupling necessary to drive the systems in a new phase. If the magnitude of the perturbation $t_y$ necessary to drive the system away from the 1D physics is small in comparison with the width of the states kept, the two-step DMRG is expected to be successful. This is, for instance, the case of coupled Haldane chains studied in Sec. IV. However, if the magnitude of the perturbation is too large, the two-step DMRG would not be able to describe the 2D physics accurately.

The real challenge in the two-step starts after finishing making the program code work. The essential part of the subsequent activity is finding a region in the parameter space of a given model where interesting physical results can be extracted. For more details about the two-step DMRG, we refer the reader to Ref. 26.

In the first step of the DMRG, we targeted charge sectors with $N_e, N_e \pm 1, N_e \pm 2$, where $N_e$ corresponds to the number of electrons at half-filling; for each charge sector, we targeted the spin sectors with the lowest $S_z, S_z \pm 1$; hence we targeted a total of $n_{\text{targ}} = 17$ charge-spin sectors during each DMRG iteration. The reduced density-matrix was given by

$$D_S = \sum_{k=1,n_{\text{targ}}} \omega_k \sum_{i_e=1,N_e} \Phi_k(S,E)\Phi_k^*(S,E), \tag{6}$$

where we assigned an equal weight $\omega_k = 1/17$ to each state $\Phi_k$. In all the simulations, we kept $ms_1 = 512$ states such that the largest truncation error was $\rho_1 \approx 10^{-6}$ for systems of up to $L_x = 32$ as can be seen in Table I.

TABLE I. Energy width $\Delta E$, truncation errors $\rho_1$ (first DMRG step), $\rho_2$ (second DMRG step) for $u = 0$, $u = 0.4261$ (near the quantum critical point), and for $u = 0.6818$ in the Hubbard lattice when $m_1 = 512$ and $m_2 = 96$ states are retained.

| | $12 \times 13$ | $16 \times 17$ | $20 \times 21$ | $24 \times 25$ | $28 \times 29$ | $32 \times 33$ |
|---|---|---|---|---|---|---|
| $\Delta E(u = 0)$ | 1.6220 | 1.2683 | 1.0410 | 0.8819 | 0.7685 | 0.6772 |
| $\rho_1(u = 0)$ | $8 \times 10^{-9}$ | $3 \times 10^{-7}$ | $7 \times 10^{-7}$ | $1 \times 10^{-6}$ | $3 \times 10^{-6}$ | $4 \times 10^{-6}$ |
| $\rho_2(u = 0)$ | 0 | 0 | 0 | 0 | 0 | $4 \times 10^{-4}$ |
| $\Delta E(u = 0.4261)$ | 1.5630 | 1.2333 | 1.0204 | 0.8733 | 0.7825 | . . . |
| $\rho_1(u = 0.4261)$ | $1 \times 10^{-7}$ | $3 \times 10^{-7}$ | $7 \times 10^{-7}$ | $1 \times 10^{-6}$ | $2 \times 10^{-6}$ | . . . |
| $\rho_2(u = 0.4261)$ | $2 \times 10^{-8}$ | $1 \times 10^{-7}$ | $3 \times 10^{-7}$ | $5 \times 10^{-7}$ | $2 \times 10^{-6}$ | . . . |
| $\Delta E(u = 0.6818)$ | 1.6249 | 1.3121 | 1.1128 | 0.9907 | 0.9134 | 0.8463 |
| $\rho_1(u = 0.6818)$ | $9 \times 10^{-8}$ | $3 \times 10^{-7}$ | $5 \times 10^{-7}$ | $1 \times 10^{-6}$ | $2 \times 10^{-6}$ | $3 \times 10^{-6}$ |
| $\rho_2(u = 0.6818)$ | $2 \times 10^{-8}$ | $8 \times 10^{-8}$ | $1 \times 10^{-7}$ | $2 \times 10^{-7}$ | $2 \times 10^{-7}$ | $7 \times 10^{-7}$ |

In the second step, we targeted $n_{\rm targ} = 3$ charge sectors $N_e, N_e \pm 1$ with the lowest $S_z$. The reduced density-matrix was formed by attributing an equal weight $\omega_k = 1/3$ for each of $k = 1, n_{\rm targ}$ states. We kept $ms_2 = 96$ states such that the width of the retained states, $\Delta E \gg t_y, t_d$ for $t_d = t_y = 0.05 t_x$. $\Delta E$ is displayed in Table I. For these parameters, the truncation error during the second step was such that $\rho_2 \lesssim \rho_1$ for systems of up to $L_x \times L_y = 32 \times 33$ when three superblock states were targeted. We empirically chose $ms_2$ such that $\Delta E/t_y = 10$. For this ratio, we can accurately reproduce the exact result at $u = 0$.

## IV. FINITE-SIZE SCALING

### A. General concepts

We apply finite-size scaling[32] to analyze the results on the charge gap $\Delta$. The procedure is simple. We accurately compute $\Delta$ in order to locate the quantum critical point. We then collapse the data using the exponents $\nu$ of known universality classes in order to find the class corresponding to the Mott transition. We emphasize that in this procedure there is no extrapolation or external parameter besides the data and the exponent of the chosen universality class.

The accurate location of the critical point is done by plotting the product $L_x^{-1}\xi$ as function of the interaction driving the transition. $\xi$ is the correlation length. This is because at the transition, $L_x^{-1}\xi$ is independent of $L_x$. For the gap, the function $L_x^{-1}\xi$ translates to $L_x^{-z}\Delta^{-1}$, where $z$ is the dynamical exponent. Near the the quantum critical point, the product $L_x^z\Delta$ is given by a universal function

$$L_x^z \Delta = f\left[(g - g_c) L_x^{1/\nu}\right], \tag{7}$$

where $g$ is a generic coupling driving the transition, $g_c$ is its magnitude at the quantum critical point, and $\nu$ is the correlation length critical exponent.

### B. Application to coupled Heisenberg chains with $S = 1$

In Fig. 2, we illustrate the finite-size analysis that we apply below to weakly coupled Heisenberg chains with $S = 1$. The model that was studied in Ref. 25 is given by the Hamiltonian

$$H_s = J_x \sum_{i_x, i_y} \mathbf{S}_{i_x, i_y} \mathbf{S}_{i_x+1, i_y} + J_y \sum_{i_x, i_y} \mathbf{S}_{i_x, i_y} \mathbf{S}_{i_x, i_y+1}. \tag{8}$$

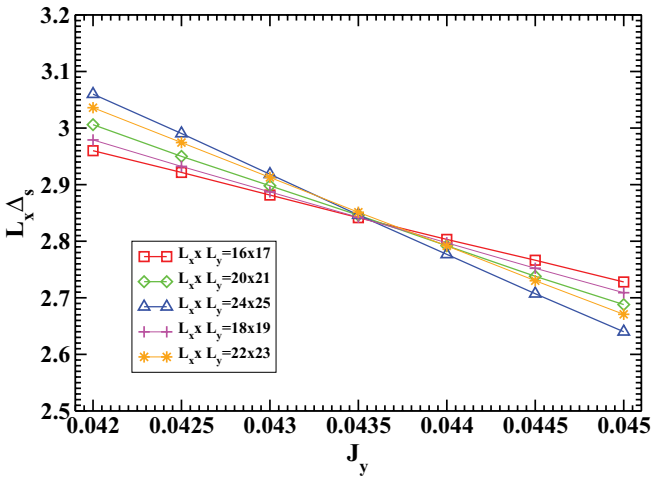


FIG. 2. (Color online) Scaled spin gap in the quasi-1D Heisenberg model as a function of $J_y$.

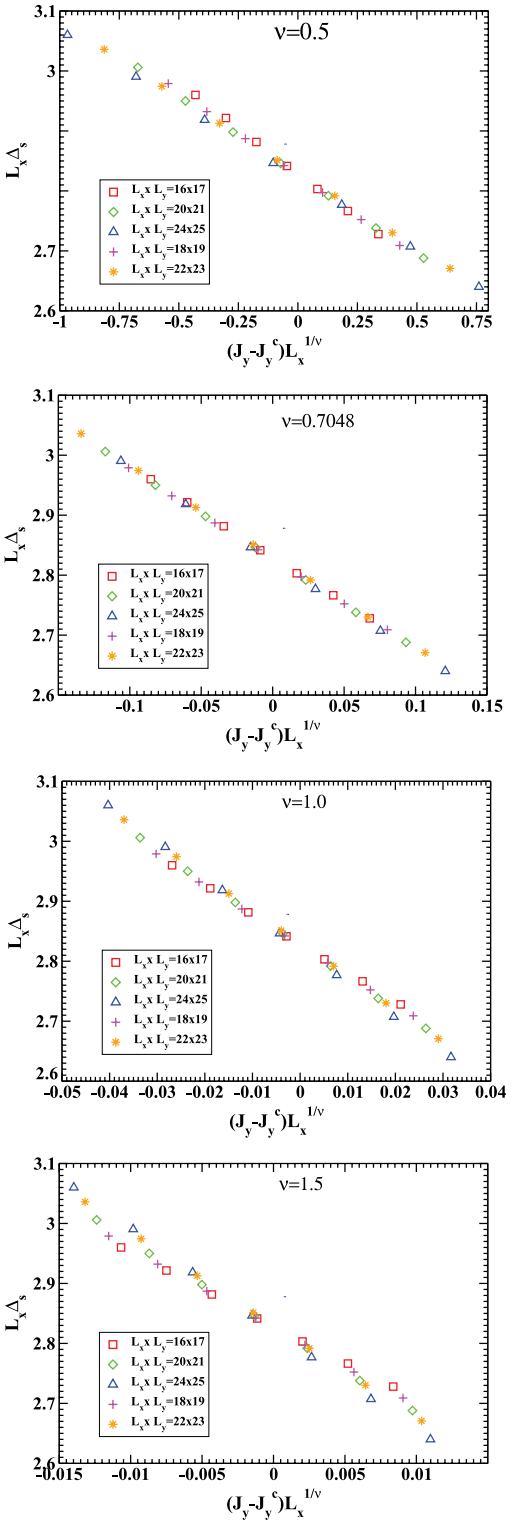


FIG. 3. (Color online) $\Delta \times L_x$ as a function of $(J_y - J_y^c)L_x^{1/\nu}$ for different $L_x \times L_y$ and for different universality classes: mean-field ($\nu = 0.5$), classical 3D Heisenberg ($\nu = 0.7048$), 2D Ising ($\nu = 1.0$), and a fictitious case ($\nu = 1.5$).

In the model (8), there is transition from a magnetically disordered ground state, the Haldane gap phase, to a magnetically ordered ground state, which is induced by the transverse coupling $J_y$. This transition has been studied by the quantum Monte Carlo method.[28] In this transition, $z = 1$, and it belongs to the universality class of the 3D classical Heisenberg model for which $\nu = 0.7048$.[33] In Fig. 2, we plot $L_x\Delta_s$ as function of $J_y$, where $\Delta_s$ is the spin gap. We studied systems ranging from $L_x \times L_y = 12 \times 13$ to $24 \times 25$. We applied periodic boundary conditions along the $x$ direction and open boundary conditions along the $y$ direction. At the quantum critical point, $J_y = J_y^c$, $L_x\Delta_s$ is independent of $L_x$. There are small size effects for smaller systems. We thus included only systems larger than $16 \times 17$. All the curves $L_x\Delta_s$ cross at $J_y^c$. The critical point $J_y^c = 0.043\,68$ was located graphically. It is in perfect agreement with the quantum Monte Carlo value $J_y^c = 0.043\,648(8)$.

The determination of the universality class is done by plotting $L_x\Delta_s$ as function of $(J_y - J_y^c)L_x^{1/\nu}$. In Fig. 3, $L_x\Delta_s$ is displayed for different values of $\nu$ corresponding to mean-field, classical 3D Heisenberg, 2D Ising, and a fictitious universality class with $\nu = 1.5$. As expected from Monte Carlo simulations, the best data collapse was obtained for $\nu \approx 0.7048$ which is predicted Monte Carlo value[33] for the classical 3D Heisenberg universality class.

## V. RESULTS AND DISCUSSION

We can now confidently apply the same method to the Hubbard model. First, we compared the two-step DMRG results with the exact energies at $u = 0$. We emphasize that this test is nontrivial for a real-space technique such as the DMRG because in real space, the hopping term is nondiagonal. In Fig. 4(a), we show the error $\delta E$ in the ground-state energies per site for systems ranging from $L_x \times L_y = 12 \times 13$ to $32 \times 33$. The two-step DMRG is in very good agreement with the exact result; $\delta E < 10^{-6}$ and increases relatively slowly with $L_x$ for systems $L_x \times L_y < 28 \times 29$ and starts to grow sharply beyond this size. In Fig. 4(b), we compare the single-particle gap, $\Delta = \frac{1}{2}[E_0(N+1) + E_0(N-1) - 2E_0(N)]$, obtained with the two-step DMRG to the exact gap. The largest error for the gap was about $5 \times 10^{-4}$ in the $32 \times 33$ systems. Since for this size the exact gap is only $\Delta = 0.001\,03$, we excluded the $32 \times 33$ systems from the data used to extract the critical exponent. For the largest systems kept for the analysis $28 \times 29$, the two-step DMRG gap is $\Delta = 0.008\,95$ which is

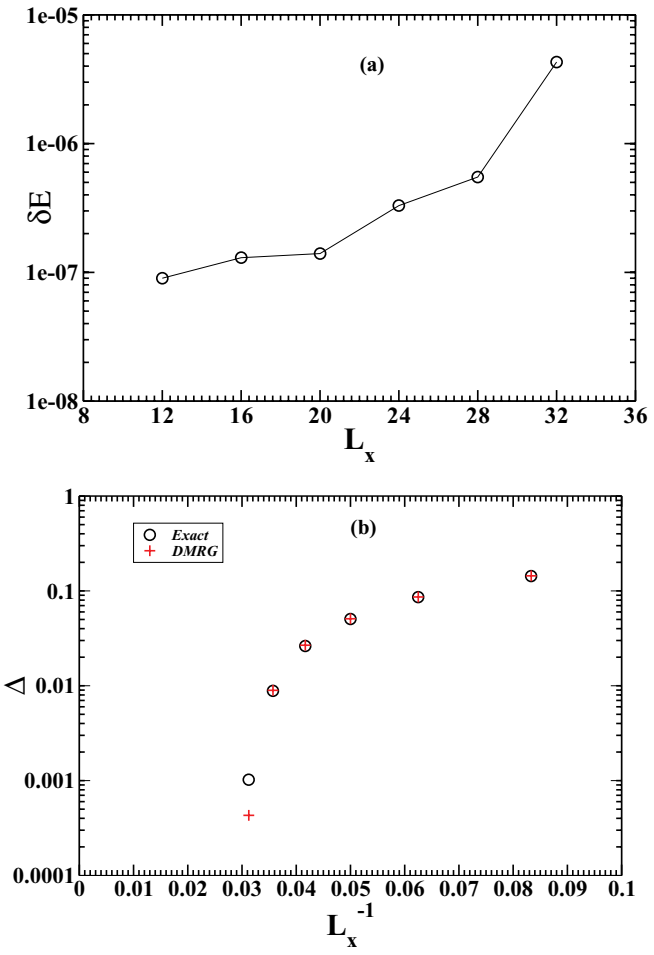


FIG. 4. (Color online) Error in the ground-state energy for quasi-one-dimensional systems as a function of the linear dimension $L_x$ of the lattice. Single-particle two-step DMRG gaps vs exact gaps as function of $L_x$.

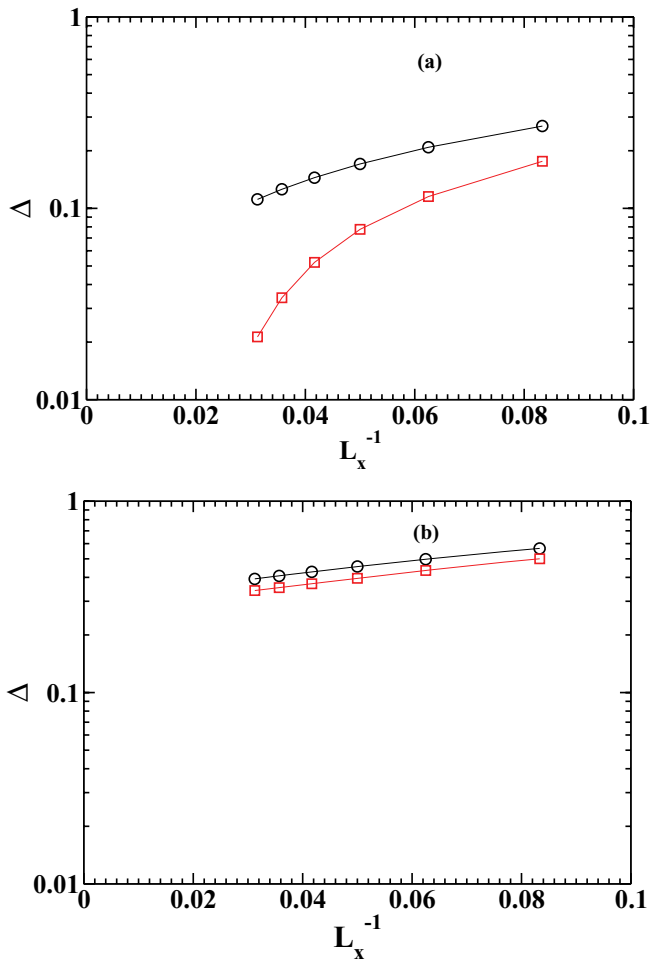


FIG. 5. (Color online) Quasiparticle gaps as a function of $L_x$ for two characteristic values of the interaction: (a) $u = 0.2273$, (b) $u = 0.6818$ for 1D (circles), and quasi-1D (squares) systems.

to be compared to the exact gap $\Delta = 0.008\,83$. The relatively large loss of accuracy in the gap for $32 \times 33$ systems follows from the sharp increase in $\delta E$.

When $u \neq 0$, the two-step DMRG retains the same level of accuracy as at $u = 0$. This is because, when the same number of states $m_2$ is kept, the truncation error $\rho$ remains close to that of $u = 0$ as seen in Table I. $\Delta E$ slightly increases with $u$, hence, the condition $\Delta E \gg t_y, t_d$ is also fulfilled. Unlike the pure 1D model, the metallic phase is expected to have a finite width in the quasi-1D model. In Fig. 5, we show the gap as a function of $L_x$ for two characteristic values of the interaction at $u = 0.2273$ and $u = 0.6818$ for the 1D and quasi-1D systems. There appear to be two regimes. In Fig. 5(a), for $u = 0.2273$, the quasi-1D gap shows a sharp decay in contrast to the 1D gap which decays more slowly. This is consistent with the finite value of the 1D gap and the presumably zero value of the quasi-1D gap in the thermodynamic limit. In Fig. 5(b), for $u = 0.6818$, both gaps remain very close and have a finite value in the thermodynamic limit. This behavior suggests that there would be a quantum critical point at $0.2273 \lesssim u_c \lesssim 0.6818$. We would like to emphasize that in Ref. 25, in 1D in agreement with the exact result[4] the DMRG yielded $u_c = 0$.

We analyze our results using the language of second order transitions. This is justified because we did not see any sharp change in our data for the ground-state energy or the gap. Generally, in a first-order transition, it would usually be expected that the ground-state energy would be nondifferentiable and the gap would show a discontinuity at the transition point. These were not seen in our data. The absence

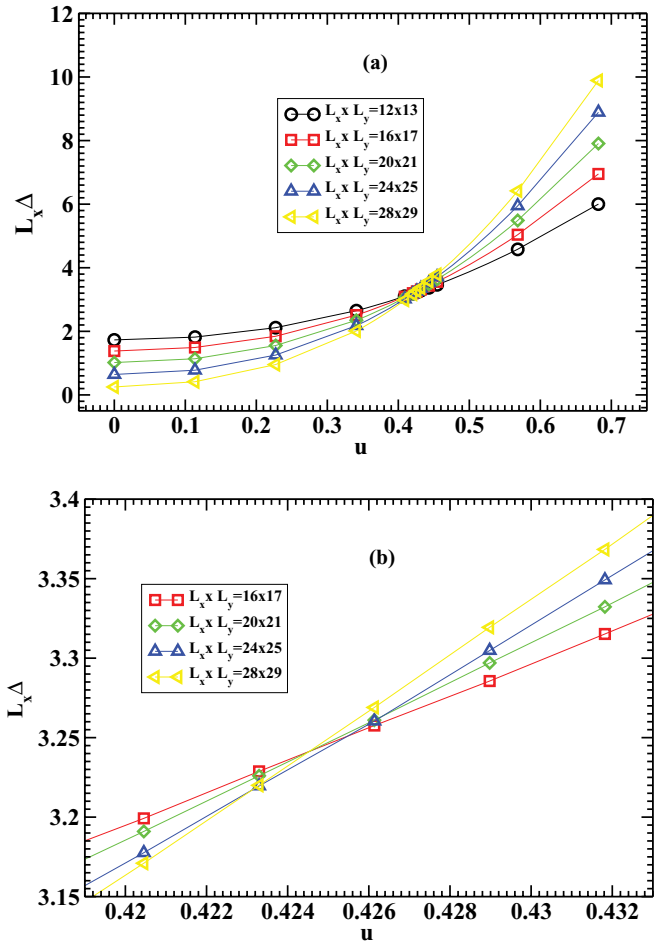


FIG. 6. (Color online) $\Delta \times L_x$ as function of $u$ for the Hubbard model: (a) extendend range of $u$, (b) for $u$ in the vicinity of the quantum critical point.

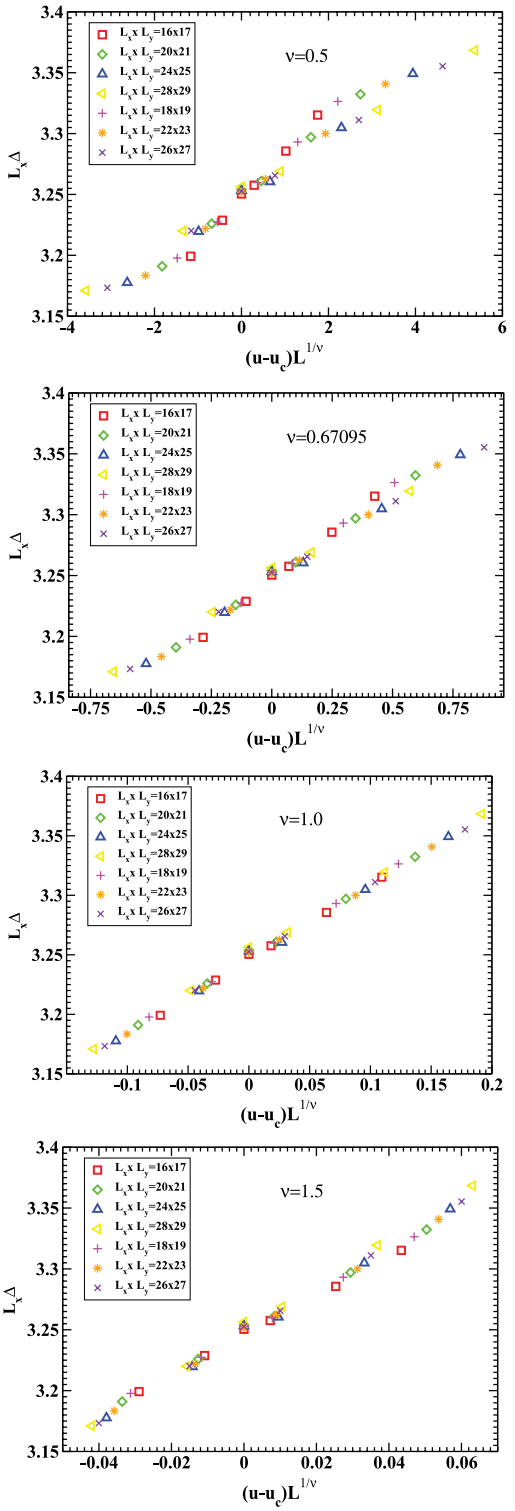


FIG. 7. (Color online) $\Delta \times L_x$ as a function of $(u - u_c)L_x^{1/\nu}$ for different $L_x \times L_y$ for $\nu$ corresponding to different universality classes: mean-field ($\nu = 0.5$), 3D classical $XY$ ($\nu = 0.670\,95$), 2D Ising ($\nu = 1.0$), and fictitious ($\nu = 1.5$).

of a discontinuity is seen for instance in the behavior of $L_x\Delta$ in Fig. 6. This justifies the assumption that the transition is of second order.

As for the Heisenberg model above, in Refs. 17 and 18, the value $z = 1$ was predicted for the interaction induced Mott transition. But in the density induced transition, the dynamical exponent is $z = 2$. In order to find the value of $z$, we plotted both $L_x\Delta$ and $L_x^2\Delta$. However, the rough estimate of the critical value found for $L_x^2\Delta$, $u_c \approx 0.1705$ was very inconsistent with the direct extrapolation of the data. For instance, at $u = 0.2273$, $\Delta$ extrapolates to 0. This allows us to rule out $z = 2$ as well as higher values of $z$ since they yield even smaller $u_c$.

We show for $z = 1$, $L_x\Delta$ as function of $u$ in Fig. 6. A first sweep of the interaction range $0 \leqslant u \leqslant 0.6818$ in Fig. 6(a) indicates that $0.4 \leqslant u_c \leqslant 0.5$. In Fig. 6(b), to precisely locate $u_c$, we concentrate in the interaction range $0.420 \leqslant u \leqslant 0.432$, a graphical estimate yields $u_c = 0.4255$. The range of values of $u$ for the critical analysis $\delta u = 0.02656u_c$ is comparable to that used in Ref. 17 $|\delta(J/U)| = 0.015\,26(J/U)_c$ for the Bose Hubbard model, and in Ref. 18 $|\delta(t/g)| = 0.013\,39(t/g)_c$ for the Jaynes-Cummings-Hubbard model. $(J/U)$ and $t/g$ are the ratio of the hopping parameter over the interaction.

As for the Heisenberg model above, we determine the universality class of the Hubbard model by plotting $L_x\Delta$ as function of $(u - u_c)L^{1/\nu}$. In Fig. 7, we tried different values of $\nu$ corresponding to the mean-field $\nu = 0.5$, 3D $XY$, 2D Ising $\nu = 1.0$, and a fictitious $\nu = 1.5$ cases. For the 3D $XY$ model, Monte Carlo values $\nu$ are found between $\nu = 0.662(7)$ and 0.6723,[34] and with the bosonic Hubbard model[17] and the Jaynes-Cummings-Hubbard model[18] for which $\nu = 0.6715$. The experiments on $H_e^4$ films are believed to yield the best estimate of $\nu$ for the 3D $XY$ models. Experiments have smaller errors than Monte Carlo simulations. For instance, $\nu$ was found to be $\nu = 0.6708(4)$ in Ref. 35, $\nu = 0.6705(6)$ in Ref. 36, and $\nu = 0.670\,95(13)$ in Ref. 37. We used this last value to collapse the data for the test of the 3D $XY$ universality class.

Figure 7 clearly shows that the best fit to the data is obtained for $\nu = 1.0$. This implies that the Mott transition in the Hubbard model belongs to the universality class of the 2D Ising model as predicted by the approximate mapping of Ref. 23.

The 3D $XY$ universality class for the Mott transition in 2D was conjectured in approximate slave-rotor analyses of the fermionic Hubbard model in Refs. 21 and 22. This work shows that the neglect of the gauge field during the factorization of the fermionic operators into a spinless boson and a charge-less spin is not justified. It should be noted that the 3D Ising and 3D Heisenberg universality class for which $\nu$ is close to that of the 3D $XY$ class, respectively, $\nu = 0.6298(5)$[38] and $\nu = 0.7048$[33] were also ruled out.

## VI. CONCLUSION

In this paper, we used the two-step DMRG to analyze the finite size behavior of the quasiparticle gap in the ground-state Mott transition in the quasi-1D Hubbard model. We chose a nonbipartite lattice to avoid the issue related to the possible nesting induced Slater transition. We studied systems ranging from $12 \times 13$ to $32 \times 33$. We believe that there are not significant finite size effects in our work as seen from the quality of the data collapse. The most solid evidence supporting our work is the preliminary analysis of the paramagnetic-antiferromagnetic transition in quasi-1D Heisenberg systems. In this analysis, the critical transverse coupling is $J_y = 0.043$, which is of the same order with $t_y = 0.05$ in the quasi-1D Hubbard. We studied nearly the systems with the same sizes in the two transitions. In both transitions, the gap at the transition has a power law behavior with $\nu = 0.7$ and 1, respectively. We were thus able to find the universality class of the Mott transition in an unbiased calculation.

In contrast to the pure 1D model, we find that the quasi-1D models displays a genuine Mott transition at a finite critical interaction. Moreover, the quasi-1D solution does not have the pathologies of the infinite dimensional solution. It could thus serve as a basis for more realistic studies of the detailed and well controlled analysis of the Mott transition. The critical behavior of the quasi-1D model Hubbard model is found to belong to the universality class of the 2D Ising model. The fact that the transitions in the quasi-1D Heisenberg and Hubbard models belong to the universality classes of their isotropic counterparts shows that despite the restriction of the two-step DMRG method to highly anisotropic 2D models, it is nevertheless very useful for the understanding of the physics of isotropic 2D systems.

We did not discuss the spin degrees of freedom. They are expected to be gap-less in either side of the Mott transition. Spin fluctuactions are expected to be very strong in the Mott insulating phase as well as in the metallic phase in the vicinity of the quantum critical point. The simplest ground-state picture is that the antiferromagnetic transition takes place at the same point as the Mott transition. But there is alternative possibility of intermediate phases between the Fermi liquid and the antiferromagnetic Mott insulator. In the metallic region, this could be a non-Fermi liquid as the one discussed in Ref. 39. In the insulating region, a gap-less spin liquid ground state with a spinon Fermi surface as suggested in Refs. 21 and 22 could be the most stable. The isomorphism $SU(2)/Z_2 \equiv SO(3)$ implies that, in principle, after the Mott transition which involves the breaking of a $Z_2$ Ising symmetry, the effective spin Hamiltonian, obtained by projecting out the empty and doubly occupied states, can retain the full spin SO(3) spin rotational symmetry.

## ACKNOWLEDGMENTS

This work was supported in part by a Shapira fellowship of the Israeli Ministry of Immigrant Absorption (S.M.) and by the Israel Science Foundation through Grant No. 1524/07.

[1] N. F. Mott, Proc. Phys. Soc. London, Sect. A **62**, 416 (1949).
[2] M. Imada, A. Fujimori, and Y. Tokura, Rev. Mod. Phys. **70**, 1039 (1998).
[3] J. Hubbard, Proc. R. Soc. London A **277**, 237 (1964).
[4] E. H. Lieb and F. Y. Wu, Phys. Rev. Lett. **20**, 1445 (1968).
[5] W. Metzner and D. Vollhardt, Phys. Rev. Lett. **62**, 324 (1989).

[6]A. Georges and G. Kotliar, Phys. Rev. B **45**, 6479 (1992).
[7]A. Georges, G. Kotliar, W. Krauth, and M. J. Rozenberg, Rev. Mod. Phys. **68**, 13 (1996).
[8]S. Moukouri and M. Jarrell, Phys. Rev. Lett. **87**, 167010 (2001).
[9]O. Parcollet, G. Biroli, and G. Kotliar, Phys. Rev. Lett. **92**, 226402 (2004).
[10]T. Maier, M. Jarrell, T. Pruschke, and M. H. Hettler, Rev. Mod. Phys. **77**, 1027 (2005).
[11]Y. Z. Zhang and M. Imada, Phys. Rev. B **76**, 045108 (2007).
[12]T. Ohashi, T. Momoi, H. Tsunetsugu, and N. Kawakami, Phys. Rev. Lett. **100**, 076402 (2008).
[13]H. Park, K. Haule, and G. Kotliar, Phys. Rev. Lett. **101**, 186403 (2008).
[14]N. Balzer, B. Kyung, D. Sénéchal, A.-M. S. Tremblay, and M. Potthoff, Europhys. Lett. **85**, 17002 (2009).
[15]M. P. A. Fisher, P. B. Weichman, G. Grinstein, and D. S. Fisher, Phys. Rev. **40**, 546 (1989).
[16]N. Elstner and H. Monien, Phys. Rev. **59**, 12184 (1999).
[17]B. Capogrosso-Sansone, S. G. Soyler, N. Prokof'ev, and B. Svistunov, Phys. Rev. A **77**, 015602 (2008).
[18]M. Hohenadler, M. Aichhorn, S. Schmidt, and L. Pollet, Phys. Rev. A **84**, 041608(R) (2011).
[19]J. E. Hirsch, Phys. Rev. B **31**, 4403 (1985).
[20]C. N. Varney, C.-R. Lee, Z. J. Bai, S. Chiesa, M. Jarrell, and R. T. Scalettar, Phys. Rev. B **80**, 075116 (2009).
[21]S. Florens and A. Georges, Phys. Rev. B **70**, 035114 (2004).
[22]T. Senthil, Phys. Rev. **78**, 045109 (2008).
[23]C. Castellani, C. Di Castro, D. Feinberg, and J. Ranninger, Phys. Rev. Lett. **43**, 1957 (1979).
[24]M. Blume, V. J. Emery, and R. B. Griffiths, Phys. Rev. A **4**, 1071 (1971).
[25]S. Moukouri and E. Eidelstein, Phys. Rev. **84**, 193103 (2011).
[26]S. Moukouri, Phys. Rev. B **70**, 014403 (2004).
[27]N. E. Bickers and S. R. White, Phys. Rev. B **43**, 8044 (1991).
[28]M. Matsumoto, C. Yasuda, S. Todo, and H. Takayama, Phys. Rev. **65**, 014407 (2001).
[29]S. R. White, Phys. Rev. Lett. **69**, 2863 (1992).
[30]S. Drell, M. Weinstein, and S. Yankielowicz, Phys. Rev. D **14**, 487 (1976).
[31]K. G. Wilson, Rev. Mod. Phys. **47**, 773 (1975).
[32]M. N. Barber, in *Phase Transitions and Critical Phenomena*, edited by C. Domb and J. L. Lebowitz, Vol. 8 (Academic Press, London, 1983), p. 145.
[33]K. Chen, A. M. Ferrenberg, and D. P. Landau, Phys. Rev. **48**, 3249 (1993).
[34]M. Hasenbusch and T. Török, J. Phys. A **32**, 6361 (1999).
[35]D. R. Swanson, T. C. P. Chui, and J. A. Lipa, Phys. Rev. **46**, 9043 (1992).
[36]L. S. Goldner, N. Mulder, and G. Ahlers, J. Low Temp. Phys. **93**, 131 (1993).
[37]J. A. Lipa, D. R. Swanson, J. A. Nissen, T. C. P. Chui, and U. E. Israelsson, Phys. Rev. Lett. **76**, 944 (1996).
[38]M. Hasenbusch, K. Pinn, and S. Vinti, Phys. Rev. B **59**, 11471 (1999).
[39]S. Moukouri and E. Eidelstein, Phys. Rev. B **82**, 165132 (2010).